Partition function, metastability, and kinetics of the escape transition for an ideal chain

L. I. Klushin*

The American University of Beirut, Department of Physics, Beirut, Lebanon

A. M. Skvortsov

Chemical Pharmaceutical Academy, Prof. Popova 14, 197022, St. Petersburg, Russia

F. A. M. Leermakers

Laboratory of Physical Chemistry and Colloid Science, Wageningen University, Dreijenplein 6, 6703 HB Wageningen, The Netherlands.

An end-tethered polymer chain squeezed between two pistons undergoes an abrupt transition from a confined coil state to an inhomogeneous flower-like conformation partially escaped from the gap. We present a rigorous analytical theory for the equilibrium and kinetic aspects of this phenomenon for a Gaussian chain. Applying the analogy with the problem of the adsorption of an ideal chain constrained by one of its ends, we obtain a closed analytical expression for the exact partition function. Various equilibrium thermodynamic characteristics (the fraction of imprisoned segments, the average compression, and lateral forces) are calculated as a function of the piston separation. The force versus separation curve is studied in two complementary statistical ensembles, the constant force and the constant confinement width ones. The differences in these force curves are significant in the transition region for large systems, but disappear for small systems. The effects of metastability are analyzed by introducing the Landau free energy as a function of the chain stretching, which serves as the order parameter. The phase diagram showing the binodal and two spinodal lines is presented. We obtain the barrier heights between the stable and metastable states in the free energy landscape. The mean first passage time, i.e., the lifetime of the metastable coil and flower states, is estimated on the basis of the Fokker-Planck formalism. Equilibrium analytical theory for a Gaussian chain is complemented by numerical calculations for a lattice freely jointed chain model.

PACS number(s): 05.40.−a, 05.70.Fh

I. INTRODUCTION

Phase transitions in macromolecular systems can be fundamentally divided into two classes. The first class occurs in the condensed bulk matter, involves a macroscopically large number of molecules, and is basically similar to that in ordinary fluids or solids. The size of a single molecule plays only a minor role in the nature of these transitions at least as far as the equilibrium aspects are concerned. Crystallization, segregation of incompatible liquids, and liquid-crystalline ordering can serve as examples [1–3]. The second class of phase transitions belongs exclusively to the realm of polymers since it is realized at the level of a single macromolecule and does not have any analogy in the physics of low molecular mass systems. The best-known examples are the coil-globule [4] and coil-stretch [5] transitions, as well as adsorption at a solid-liquid interface [6,7].

The concept of a phase transition always requires one to be in the thermodynamic limit. When the first derivatives of the free energy change jumpwise at the transition one has to do with a transition of the first-order type. First-order phase transitions have a more gradual character in small systems,

e.g., when there is a specific geometry with a large surface-to-volume ratio. A phase transition on the level of a single molecule is therefore not obvious; a single macromolecule always consists of a finite number of segments, usually $N \sim 10^2 - 10^6$, so that finite-size effects in single-molecule phase transitions are the rule rather than the exception. As a result, in real systems the phase transition must remain smooth. However, if in the (academic) limit of infinite length of the chain the transition becomes first order, one usually still refers to the transition as first-order-like, even for finite N.

The goal of this paper is to present a rigorous analytical theory for a phase transition in a single macromolecule that has received much attention recently, namely the escape transition observed for an end-tethered chain compressed between two pistons [8–18]. At weak compressions, the chain is deformed uniformly to make a relatively thick pancake; the resistance force due to the compressed chain increases monotonously as the distance between two pistons, H, decreases. Beyond a certain critical compression, the chain changes conformation abruptly. One part of the chain forms a stem stretching from the anchoring point to the piston edge, while the remainder of the chain forms a coiled crown outside the pistons, thus escaping from underneath the piston. The resistance force decrease abruptly, indicating a first-order transition.

First-order transitions are associated with the existence of metastable states that are stable with respect to small fluc-

*On leave from the Institute of Macromolecular Compounds of the Russian Academy of Sciences, Bolshoy prospect 31, 199004, St. Petersburg, Russia.

tuations. A metastable state decays with a finite rate, which is mostly controlled by the nucleation barrier. Metastable states are especially important for polymer systems. The relaxation of a metastable conformation involves the reorganization of many segments of the chain, which makes it intrinsically slow. A rigorous description of metastable states in polymer systems that suffer a transition is an outstanding problem of statistical physics. The difficulty lies in finding the stable and metastable domains in a multidimensional phase space and obtaining the height of the barrier that separates them. A strategic direction in treating these problems is to select an order parameter and to construct with this the Landau free energy. Typically, the order parameter has to be defined as a local fluctuating quantity and the Landau free energy is a functional of this order parameter field. According to the fluctuation theory of phase transitions, the importance of the correlated fluctuations of the order parameter s is characterized by its relative fluctuations or the Ginzburg number Gi $=(\langle s^2 \rangle - \langle s \rangle^2)/\langle s^2 \rangle$, where the averaging is performed over the region of order r_c^3 defined by the correlation length r_c [25]. When Gi < 1, a simple mean-field approach is applicable. A very well known example is the transition to a superconducting state. In the general case of large Gi, the problem becomes very involved mathematically and requires renormalization group methods.

In contrast to classical examples of phase transitions such as liquid–gas or magnetic systems, we will argue that the escape transition can be described by a global order parameter characterizing the polymer chain as a whole, rather than one of its local properties. Defining the order parameter as a single global variable eliminates the problem of accounting for the order parameter fluctuations of various wave vector $\vec{q}$. The only fluctuations possible are also of global nature: in the language of classical examples they are characterized by $\vec{q}=0$. Although in our problem the Ginzburg number may not always be small, the fluctuations of the global order parameter can be treated exactly in a straightforward way without resorting to any approximate scheme. This approach was used for describing the coil-stretch and coil-to-flower transitions [19], and we are going to pursue this path in the present paper again.

Note that a direct analogy in a classical magnetic system with a globally defined order parameter is rather trivial since fluctuations vanish completely in the thermodynamic limit. However, a single coil-like macromolecule in solution is anomalous in the sense that its size remains strongly fluctuating (it is of the order of its size) even for $N \rightarrow \infty$ [2,3].

The equilibrium properties of the escape transition were investigated thoroughly by scaling theory [8,9], numerical calculations [10,15], and computer modeling [13,14,18]. The main result relates the critical compression distance H^* to the piston radius, L, and the chain length, Na. For ideal chains, it is given by $H^* \sim Na/L$. Excluded-volume interactions change the relationship between H^* and the N/L ratio, $H^* \sim (Na/L)^{\nu/(1-\nu)}$, where $\nu \approx 3/5$, but the nature of the transition remains the same [8,9]. In their pioneering paper based on the blob picture of the compressed and escaped phases, Subramanian *et al.* [8,9] predicted the possibility of metastable states and indicated the broad range of parameters within which these states exist. They also indicated that the

free energy barrier to be overcome by a compressed chain in order to escape is due to the elastic free energy invested in the stretching. However, the kinetic aspects of the problem were never explicitly investigated. Moreover, even the barrier height determining the lifetime of a metastable escaped flower was not discussed.

In the following, we analyze the ideal chain case, since it allows a rigorous treatment. It serves as a good starting point for understanding more general situations and the escape transition for ideal chains was investigated very thoroughly by Ennis *et al.* using numerical methods [10]. We start from an analogy between an escape transition and a coil-to-flower transition for a chain near a solid adsorbing surface to construct a closed-form analytical expression for the partition function. The equilibrium thermodynamic properties of the transition for chains of arbitrary length follow immediately from the partition function. To analyze metastable states and kinetic aspects of the phenomenon we introduce the order parameter and calculate analytically the Landau free energy. The complete phase diagram including the coexistence line and two spinodal lines follows naturally from this result. We calculate the barrier heights separating the metastable and the equilibrium states and apply the Fokker-Planck equation formalism to find analytically the mean first passage time characterizing the lifetimes of metastable states. When appropriate, numerical results obtained for the ideal freely jointed chain are presented to complement the arguments.

II. ESCAPE TRANSITION MODEL AND ITS ANALOGIES

We are dealing with an ideal Gaussian chain of N segments with the contour length Na. The chain is compressed between two pistons of radius L and end-anchored at the center of one of the piston surfaces (Fig. 1). The separation between the pistons is H.

If the piston size is so large that the chain never leaves the gap, $L > Na$, the solution for the Green's function is well-known [20]

$$G(z,z') = \frac{2a}{H} \sum_{n=1}^{\infty} \sin\left(\frac{\pi n z}{H}\right) \sin\left(\frac{\pi n z'}{H}\right) \exp -\left(\frac{\pi n R_g}{H}\right)^2 \tag{1}$$

where z and z' are the coordinates of the two chain ends along the axis normal to the piston surface, and $R_g = a\sqrt{N/6}$ is the gyration radius of the Gaussian coil. Since we are interested in the effects due to chain squeezing, the contribution of the first term in the sum is dominant. With one chain end attached at distance δ from the impenetrable surface, and the other one being anywhere, the partition function reduces to

$$Q(H,N) = \frac{4\delta}{H} \exp\left(-\frac{N}{6}\left(\frac{\pi a}{H}\right)^2\right). \tag{2}$$

Apart from the preexponential term, which can be neglected (as demonstrated by numerical estimates), the confinement effect is equivalent to introducing an effective potential per segment, $u = kT/6(\pi a/H)^2$. The nature of this effective potential is purely entropic. In the following, we use kT as the energy unit and omit it in the equations.
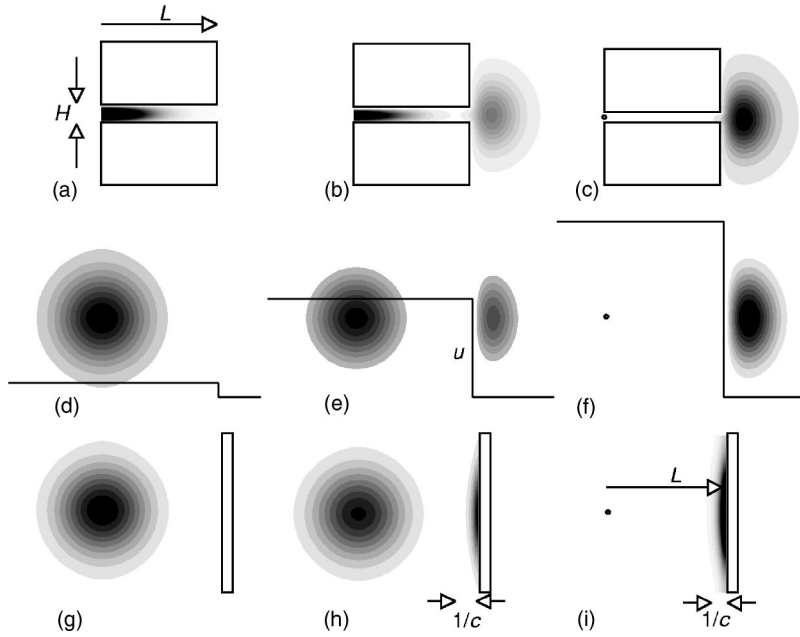
FIG. 1. Free end-point distributions as found by numerical freely jointed chain model (for details see the Appendix) without excluded volume, for three different systems featuring single chain conformational phase transitions of the coil-to-flower type. $N=425$ in all cases. A, B, C: The escape from a confinement. The chain is grafted by one end at the center of two cylindrical pistons with radius $L=45$ and separated by a distance $H=4, 5, 6$ in A, B, and C, respectively. In this example radial distributions are shown instead of a cross section. D, E, F: The escape from a stepwise external potential $u=\pi^2/(6H^2)$ with H as in A, B, C, respectively. G, H, I: The escape towards the adsorbing surface. $c=\pi/H$ with H as in A, B, C, respectively. The systems A, D, and G are the coil states. The chains in C, F, and I are in the flower conformation, whereas the systems B, E, and H are close to the transition point.

In the general case of arbitrary L and N, when the partially escaped configurations cannot be neglected, the complete solution for the Green's function is not known. It is clear, however, that the escape problem can be reduced to that of a chain in a step potential, which has a constant value u inside the gap and is zero outside (cf. Fig. 1). This analogy was first pointed out by Sevick and Williams [16].

The partition function of an end-tethered chain in a step potential was found in an integral form, but does not have a simple analytical representation [5]. However, another important analogy was established recently, namely, between a chain in the step-potential problem and a chain end-tethered at some distance away from an adsorbing solid surface [19] (cf. Fig. 1). This analogy can be easily understood in the language of effective potentials. The free energy per segment in the adsorbed part of the chain is $-(ca)^2/6$ where c is the adsorption strength parameter (the de Gennes' inverse correlation length of adsorption [3]). Hence we are once again dealing with effects similar to those of a step potential, which is zero for the part of the chain between the tethered end and the first segment in contact with the surface, and $-(ca)^2/6$ for the rest of the chain. Combining all tree analogies, we conclude that the escape problem can be reduced to the adsorption problem for a chain end-fixed at distance L from a solid surface of adsorption strength $c=\pi/H$. This reduction is especially important since the adsorption problem is the only one that admits a closed-form analytical evaluation of the partition function for chains of arbitrary length.

Mathematically, the triple analogy was firmly established [19], and we are going to exploit it extensively.

III. CLOSED FORM OF THE PARTITION FUNCTION FOR FINITE CHAINS

In the following it will be useful to introduce reduced values for the piston radius and the confinement. Both quantities will be scaled by the gyration radius of the chain, $\tilde{L}=L/2R_g$, and $\tilde{H}=H/\pi R_g$. The partition function of the adsorption problem has the following form [6,21]:

$$Q(c,L,N) = \mathrm{erf}(\tilde{L}) + \exp(-\tilde{L}^2)Y(\tilde{L}-cR_g) \qquad (3)$$

where $Y(x)=\exp(x^2)[1-\mathrm{erf}(x)]$, and $\mathrm{erf}(x)$ is the error function.

One has also to take into account the overall free energy shift, Nu, which exists for the chain between two pistons, as compared to the chain near an adsorbing surface. Finally, the partition function for the escape problem can be written as follows:

$$Q(H,L,N) = \exp(-\tilde{H}^{-2})\{\mathrm{erf}(\tilde{L}) + \exp(-\tilde{L}^2)Y(\tilde{L}-\tilde{H}^{-1})\}. \qquad (4)$$

The partition function depends explicitly only on two dimensionless scaling variables: $\tilde{L}$ and $\tilde{H}$. The quantity $\tilde{H}^{-2}$ has the interpretation of the confinement free energy, Nu, per chain in the imprisoned coil state. The analysis of the adsorption problem [22] established that there is an abrupt transition that takes place at $c^*=L/R_g^2$. In the language of the escape transition, this leads to the binodal condition

$$\frac{H^*}{a} = \frac{\pi}{6}\frac{Na}{L}. \qquad (5)$$

The transition is abrupt in the limits $\tilde{L}\gg1$ and $\tilde{H}\gg1$. The two asymptotic branches of the free energy $F=-\ln Q(H,L,N)$ are given by
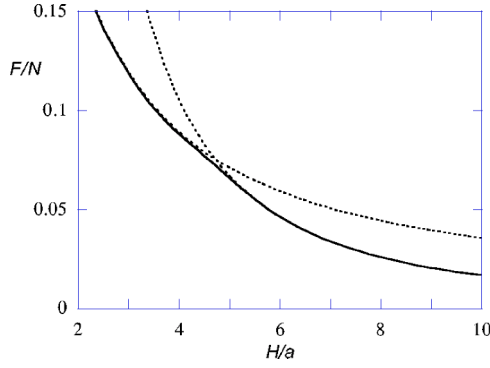
FIG. 2. Free energy per segment F/N as a function of separation distance H. Two branches of free energy corresponding to the coil state (large values of H) and the flower state (small values of H) are dotted; $L=90$; $N=800$. The branches cross at $H^*=4.65$.

$$\frac{F}{N} \approx \begin{cases} \dfrac{1}{6}\left(\dfrac{\pi a}{H}\right)^2, & H > H^* \\[3mm] \dfrac{\pi}{H}\dfrac{L}{N}, & H < H^* \end{cases} \tag{6}$$

where we see that there are two natural parameters in the system, H/a and N/L. We note that since the system is athermal, the free energy is essentially reduced to the entropic contribution. The two branches are presented in Fig. 2 for $L=90$, $N=800$. The continuations of these branches point to the possibility of metastable states. Figure 2 shows clearly the binodal point. Because of the finite length of the chain, the transition is not yet sharp.

For moderate values $\widetilde{L} \sim 1$ and $\widetilde{H} \sim 1$ all the intermediate states are important, and they are accounted for in the closed form of the partition function. Equation (4) allows for the analytical evaluation of all average characteristics of the escape transition for arbitrary chain lengths.

IV. EQUILIBRIUM CHARACTERISTICS

A. Average number of imprisoned segments

From the analogy with the chain anchored near a step-like external potential, we know that the average number of segments between the pistons, $\langle M \rangle$, can be found by considering the free energy as a function of potential per segment, u, and differentiating it with respect to u. Expressed in terms of the parameters of the escape problem, it has the following form:

$$\langle m \rangle = \frac{\langle M \rangle}{N} = 1 - \frac{\exp(-\widetilde{L}^2 - \widetilde{H}^{-2})}{Q(\widetilde{L}, \widetilde{H})}$$
$$\times \left\{ \frac{\widetilde{H}}{\sqrt{\pi}} - Y(\widetilde{L} - \widetilde{H}^{-1})(\widetilde{L}\widetilde{H} - 1) \right\} \tag{7}$$

which defines m as the fraction of confined segments. The two asymptotic branches are given by
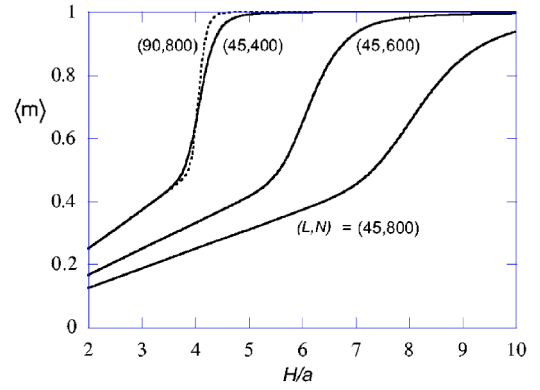

FIG. 3. Average fraction of imprisoned segments $\langle m \rangle = \langle M \rangle / N$ as a function of the confinement width H/a for $L/a=45$ and $N=400$, 600, and 800 and $L/a=90$, $N=800$ (dotted line) as indicated.

$$\langle m \rangle \approx \begin{cases} 1, & H > H^* \\[3mm] \dfrac{3H}{\pi a}\dfrac{L}{Na}, & H < H^*. \end{cases} \tag{8}$$

At the transition point $H=H^*$, $\langle m \rangle$ asymptotically jumps from the value of unity to one-half. For any finite N, the fraction of imprisoned segments at the middle point of the transition equals 2/3 to a very high accuracy.

Figure 3 demonstrates the curves $\langle m \rangle$ vs H/a for a fixed piston radius $L/a=45$ and three different chain lengths $N=400$, 600, and 800. For large piston separation, all the segments reside within the confined region. As H decreases, less segments remain inside. With increasing N the transition point shifts to larger values of H, since longer chains are easier to squeeze out. Contrary to naive expectations, the transition becomes less sharp for longer chains (at fixed L). This is due to the fact that the coil size approaches the piston size. On the other hand, if one compares the sharpness of the curves at a fixed $L/(Na)$ ratio it is clear that a larger value of N results in a sharper transition. In the thermodynamic limit $N,L \rightarrow \infty$, while keeping the ration L/N constant $\langle m \rangle$ has a jump.

B. Fluctuations of the number of imprisoned segments

Differentiating $\langle m \rangle$ with respect to u give us the reduced average square of fluctuations in the number of imprisoned segments, $\langle (\delta M)^2 \rangle / N^2$. These fluctuations are presented in Fig. 4. As far as the N-dependence is concerned, one can distinguish three different regimes. At large piston separations, when the coil is the equilibrium state, fluctuations in the number of imprisoned segments are completely negligible. Also at $H<H^*$, the equilibrium flower state results in typical fluctuations $\delta M \sim \sqrt{N}$, characteristic of standard thermodynamic behavior. Finally, near the transition point itself, the fluctuations in M are proportionate to the total number of segments, $\delta M \sim N$, and do not depend on the piston radius, L. This can be easily understood from the two-state picture, where the system fluctuates between the coil state with the fraction of imprisoned segments being equal to 1, and the flower state with the fraction of imprisoned segments being
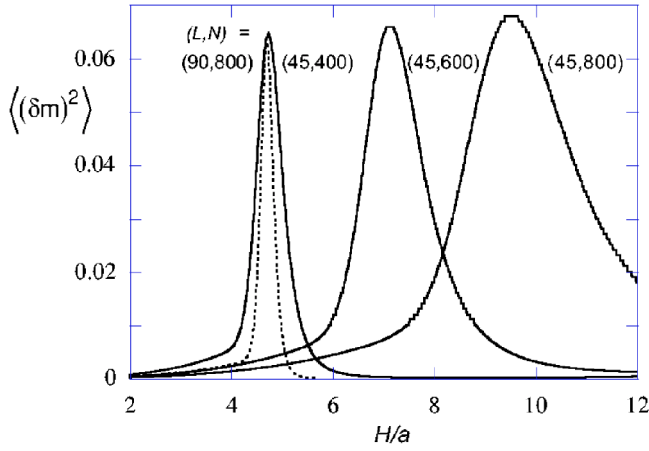
FIG. 4. Fluctuations of the fraction of imprisoned segments as a function of confinement width H/a for $L/a=45$ and $N=400$, 600, and 800 and for $L/a=90$, $N=800$ (dotted line) as indicated.

equal to $1/2$. The maximum fluctuation is achieved when these two states have equal probabilities of $1/2$, which gives $\langle(\delta M)^2\rangle=N^2/16$, which is close to the exact numerical values. If the chain length, N, is fixed, and instead the piston radius is changed, the height of the peak remains constant, while its characteristic width varies as L^{-2}.

The detailed distribution in the number of imprisoned segments was obtained earlier for the problem of the chain in a step potential [5,23,24]. The non-normalized statistical weights are given by the following expressions:

$$W(M) = \begin{cases} \dfrac{1}{\pi\sqrt{M(N-M)}}\exp\left[-\dfrac{M}{6}\left(\dfrac{\pi a}{H}\right)^2 - \dfrac{3L^2}{2M}\right], & M < N \\ \mathrm{erf}\left(\dfrac{L}{2R_g}\right), & M = N. \end{cases}$$

$$(9)$$

C. Lateral force

There exists a lateral force applied to the anchoring point where the chain end is attached to the surface of the piston. This force is given by the derivative of the free energy with respect to L:

$$f_L = \frac{\mathrm{erfc}(\tilde{L} - \tilde{H}^{-1})\exp(-2\tilde{L}\tilde{H}^{-1})}{Q(\tilde{L},\tilde{H})\tilde{H}R_g}. \qquad (10)$$

The two asymptotic branches are

$$f_L \approx \begin{cases} 0, & H > H^* \\ \dfrac{\pi}{H}, & H < H^*. \end{cases} \qquad (11)$$

At the transition point, f_L jumps from zero to La/R_g^2. Figure 5 displays the lateral force as a function of H/a for the piston sizes $L=45$ and chain length $N=200$, 400, and 800. It is clear that in the confined coil state, the lateral force vanishes. Once the escaped conformation appears, the force depends only on the confinement width but not on the chain
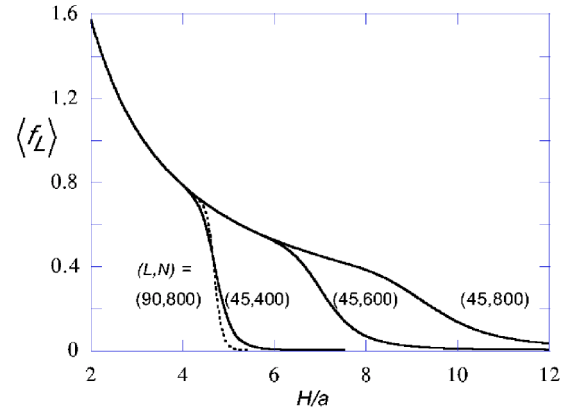

FIG. 5. Lateral force f_L as a function of confinement width H/a for $L/a=45$ and $N=200$, 400, and 800 and for $L/a=90$, $N=800$ (dotted line) as indicated.

length. One can relate the fraction of confined segments displayed in Fig. 3 with the corresponding lateral force. When all the segments reside within the confined region, the lateral force drops to zero. As H decreases, more segments escape from the confinement and the force increases. At the transition point both the lateral force and the fraction of imprisoned segments change abruptly. With increasing N the transition point shifts to larger values of H, since longer chains are easier to squeeze out. Again, the transition becomes less sharp for longer chains, which once more must be attributed to the fact that, with fixed piston dimension L and increasing values of N, the coil size approaches that of the piston. If instead one compares the sharpness of the curves at a fixed $L/(Na)$ ratio, it is clear that larger values of N result in sharper transitions.

D. Compression force

If the confinement width H is taken as an independent variable, the compression force can be obtained by differentiating the free energy $F=-\ln Q$ with respect to H:

$$\langle f_H \rangle = \frac{\pi^2 a^2}{3H^3}\langle M \rangle. \qquad (12)$$

The two asymptotic branches being:

$$f_H \approx \begin{cases} \dfrac{\pi^2 Na^2}{3H^3}, & H > H^* \\ \dfrac{\pi L}{H^2}, & H < H^*. \end{cases} \qquad (13)$$

In the thermodynamic limit, at the transition point, $H=H^*$, the force jumps from $72L^3/(\pi N^2 a^4)$ to exactly half this value.

In Fig. 6 the compression force is given for two values of L and N as indicated. Indeed there is a jump from the H^{-3} to the H^{-2} dependence exactly at the point where part of the chain escapes from the gap. Again, it is seen that at fixed ratio L/N the transition becomes more sharp with increasing chain length.
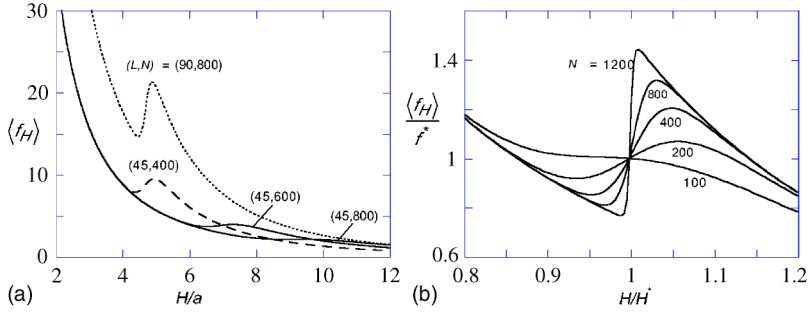
FIG. 6. (a) Average compression force $\langle f_H \rangle$ as a function of the confinement width H/a for $L/a=45$, $N=400$, 600, and 800, and $L/a=90$, $N=800$ as indicated. (b) Normalized average compression force as a function of the normalized separation, for fixed $Na/L=100/15$, for $N=100$, 200, 400, 800, and 1200 as indicated. f^* was determined from the Maxwell rule.

An important observation follows from the figures presented: in order to observe a sharp change in the properly calculated equilibrium average characteristics, very long chains are required, with N at least several hundred. This is due to the fact that squeezing a chain even down to the thickness of just 3 segment lengths results in a fairly weak effective potential per segment, $u \sim 0.14$.

Thermodynamics introduces the notion of extensive and intensive variables. As a rule, the total number of particles, N, and the total volume serve as extensive variables: This results in the well-known Gibbs-Duhem relationship for the Gibbs free energy. The system we are dealing with presently is more intricate. It is clear from Eq. (6) for the limiting form of the free energy that there is no single variable that is extensive in the whole range of parameters. Instead, each of the two branches of F has its own extensive variable: this is N for the confined coil state and L for the escaped flower state. As a result, there are two separate relationships analogous to the Gibbs-Duhem equation. For the coil state, $F=Nu(H)$, and therefore

$$\frac{\partial u}{\partial H} = \frac{f_H}{N}. \tag{14}$$

For the flower state, $F=L(\pi/H)=LF_L(H)$, which leads to

$$\frac{\partial f_L}{\partial H} = \frac{f_H}{L}. \tag{15}$$

The fact that an extensive variable does exist implies certain homogeneity of the system. One would expect this property to break down if the coil is squeezed between, e.g., curved or nonparallel surfaces.

V. ESCAPE TRANSITION IN THE CONSTANT FORCE ENSEMBLE

In the literature, there is an extensive discussion on the features of the escape transition in two different statistical ensembles: the (N,L,H) ensemble, where the confinement width serves as an independent variable, and the (N,L,f_H) ensemble, where the independent variable is the external compression force [13,14,16]. The discussion was prompted by the observation that the average compression force as a function of the confinement width, $\langle f_H \rangle (H)$, displays a nonmonotonic behavior. This nonmonotonic form of the force curve should not be identified as a van der Waals loop; the force curve crosses the binodal just once, at the transition

point. In other words, the polymer is at each moment during the escape transition in either the coil or in the flower state, but these two states never coexist simultaneously [16]. It was argued though, that in the (N,L,f_H) ensemble (where the compression force is fixed) the curve of the average separation, $\langle H \rangle$, versus f_H will contain a vertical segment [13,14,16]. Of course, this is not possible as we will show below.

A naive thermodynamic consideration concludes that the relevant potentials for the two ensembles (the Gibbs and the Helmholtz free energies) are related to each other by a Legendre transformation:

$$G(N,L,f_H) = F(N,L,H) + f_H H. \tag{16}$$

From the two asymptotic branches of the Helmholtz energy, F, given by Eq. (6), and the force, f_H, [Eq. (13)], one obtains

$$G(N,L,f_H) = \begin{cases} \frac{1}{2}N^{1/3}(3\pi f_H)^{2/3}, & f_H < f^* \\ 2(\pi L f_H)^{1/2}, & f_H > f^*. \end{cases} \tag{17}$$

The two branches match at $f^* = (\frac{8}{3})^4 L^3/(\pi N^2 a^4)$, this automatically satisfies the Maxwell's rule for the $\langle f_H \rangle$ vs H isotherm, see Fig. 6.

Of course this approach fails to incorporate finite-size effects. The complete description must be based on the relationship between the partition functions rather than the thermodynamic potentials.

To find the partition function for the (N,L,f_H) ensemble one has to take the number of configurations at a given value of H, include the Boltzmann weight associated with the external force, $\exp(-f_H H)$, and integrate over all values of the piston separation H:

$$Q_G(N,L,f_H) = \int_0^\infty Q(N,L,H)\exp(-f_H H)dH. \tag{18}$$

The Legendre transformation (16) for the thermodynamic potentials follows from this general expression only in the limit when the integral is reduced to the single contribution at the maximum of the integrand.

The average width $\langle H \rangle$ is given by

$$\langle H \rangle = \frac{1}{Q_G} \int_0^\infty Q(N,L,H)\exp(-f_H H)HdH. \tag{19}$$
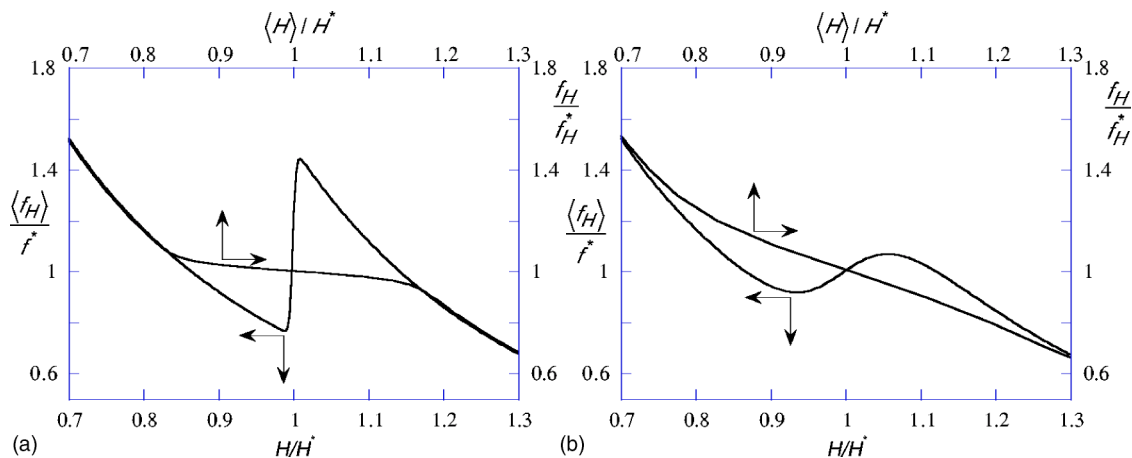
FIG. 7. Scaled average confinement force $\langle f_H/f^* \rangle/H^*$ (left y axis) as a function of the normalized confinement width H/H^* (bottom x axis) as well as the scaled average confinement width $\langle H/H^* \rangle$ (top x axis) as a function of the scaled compression force f_H/f^* (right y axis) for $Na/L=100/15$: (a) $N=1200$ and (b) $N=200$.

Figure 7 demonstrates how one and the same phenomenon (escape transition) occurs in complementary ensembles both in large and in small systems. In this graph we present on the left y axis the average compression force normalized to f^*, which is a function of the normalized confinement width (bottom x axis). In the complementary force ensemble the average confinement $\langle H \rangle$ normalized to H^* (top x axis) is found as a function of the confinement force (right y axis). Both sets of graphs in panels (a) and (b) correspond to the same ratio $L/Na=0.15$, but in Fig. 7(a) the system is much closer to the thermodynamic limit as $N=1200$ as compared to the length of the chain $N=200$ for Fig. 7(b).

From Fig. 7 two observations can be made. First, the two ensembles are not equivalent in the vicinity of the transition. The average normalized force jumps by a factor of 2 from $3^6/2^9$ to $3^6/2^{10}$ but the normalized average distance drops from $72/64$ to a value $54/64$. Out of the transition region $(54/64)H^* < H < (72/64)H^*$ the two ensembles give the same force-distance relation.

Second, for small systems the difference between the force-distance curves obtained in the two ensembles gradually disappears also in the transition region.

The discussion of the picture of the escape transition in two ensembles was originally motivated by the analogy with the gas–liquid transition. It was noted already that this analogy is not quite straightforward: for the escape transition, one cannot speak of a simultaneous coexistence of two phases in the same sense as coexisting liquid and vapor within the same vessel [25].

A. End-point distributions by numerical lattice calculations

In order to obtain some more detailed information on the escape problem and to establish the validity range of the analytical theory for Gaussian chains based on the analogy with the adsorption and the step-potential problems we have performed numerical calculations for a freely jointed chain model on a cylindrical lattice that takes into account the exact piston geometry. For details we refer to the Appendix.

In particular, we generate the radial end-point distribution functions and analyze the way they change as a function of the piston size L/a, Fig. 8 (in Fig. 1 results are shown for the case that H/a was varied at fixed L/a). For $N=400$ and $H=5a$, the chain is clearly confined when $L\geq 46a$. For $H\leq 44a$, the chain takes a partially escaped conformation as the probability of the chain end to remain in the gap between the pistons becomes a minority. $L=45a$ seems to be close to the transition point. The distribution is clearly bimodal suggesting the existence of two sets of conformations, and the two peaks are approximately of the same height. For the parameters chosen, the analytical theory predicts the binodal at $H^*=4.65a$, which is very close (one has to keep in mind some arbitrariness that exists in lattice models when dealing with distances less than the lattice constant). Bimodality of the distribution exists for other values of H/a as well, although it can be discerned only on a log scale. For $H>8a$, the local maximum corresponding to the end positions outside the slit disappears suggesting that the flower state becomes completely unstable.

The position of the free end may be considered as a candidate for the order parameter. Then, the logarithm of the end distribution will give the Landau free energy. However, this
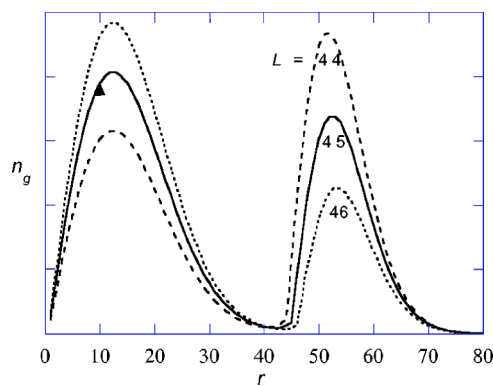

FIG. 8. End-point distribution for freely jointed chain with $H=5$ and $N=400$, for various values of the piston size L as indicated.

choice fails to fulfill a certain natural requirement, as discussed in the next section.

B. Order parameter and Landau function

The exact partition function contains contributions from all chain configurations including those associated with metastable states (provided the parameter values allow metastability). However, these contributions are masked, and one has to take special care in order to single them out and analyze metastable states *per se*. The approach of the Landau theory is ideally suited specifically for this task. In the Landau theory, all the configurations are first subdivided into sets associated with a given value of the order parameter, s, and summation is performed separately within each set. The full partition function can be obtained then by integrating over the order parameter:

$$\exp - F = \int ds \, \exp[-N\Phi(s)] \tag{20}$$

where $\Phi(s)$ is the Landau function, that is, the nonequilibrium free energy taken as a function of the order parameter. In the close vicinity of the transition point, the Landau free energy is expected to have two minima (one stable and the other metastable). Our analysis will be focused on finding the metastable minima and the associated thermodynamic characteristics, as well as the height of the barrier separating the local minimum from the global one which determines the lifetime of the metastable state.

The proper choice of the order parameter is not always obvious, nor are there any standard recipes for making it. One criterion is quite clear: the average value of the order parameter should allow one to distinguish between two phases. For a first-order transition, the average order parameter changes jumpwise. We require that the properly chosen order parameter changes continuously as the system evolves from a metastable state, through the transition state at the top of the barrier, and eventually falls into the equilibrium minimum. As a response to the confinement H, the ideal coil state is perturbed. Before the chain can escape from the unfavorable state, it must be stretched to reach the region outside the pistons. A seed crown is formed that grows subsequently at the expense of the stem until the equilibrium state is reached. In this process, it is the chain stretching parameter that grows continuously. For the deformed coil, the parameter refers to the chain as a whole, $s = r_N / Na$, where $r_N = \sqrt{x_N^2 + y_N^2}$ is the radial distance from the center of the piston (anchoring point). However, using the chain end position as the order parameter for the flower state is not appropriate: The resultant average order parameter for flower conformations turns out to be independent of the magnitude of the effective fields, u. Thus it cannot discriminate between various flower conformations. Since the field magnitude affects the stretching of the stem, we choose the order parameter in the flower conformation as the stretching of the stem only: $s = L / na$, where n is the number of segments in the stem. The two definitions match smoothly at $r_N = La$, $n = N$.

Accordingly, the Landau function consists of two branches that have to be introduced separately. Our calcula-

tions are based on the step-potential analogy suggested by Sevick and Williams [16]. The coil branch is defined as $\Phi_{\text{coil}}(s) = -\frac{1}{N}\ln G_{\text{coil}}(s)$, where $G_{\text{coil}}(s)$ is the Green's function of the coil between pistons with one end fixed at $r = 0$ and the other end at $r_N = sNa$ calculated under condition that no segment extends beyond $r = L$. This is ensured by imposing a vanishing boundary condition at a fictitious surface placed at distance $r = L + \delta$. Utilizing the results of the standard reflection method for a 1D problem, the solution for the cylindrical geometry can be written as

$$G_{\text{coil}}(r_N) = \frac{3r_N}{Na^2}\exp\left(-\frac{3r_N^2}{2Na^2} - Nu\right)\left\{1 - \left(1 - \frac{6\delta L}{Na^2}\right) \\ \times \exp\left[-6\frac{L}{Na^2}(L - r_N)\right]\right\}. \tag{21}$$

Taking $\delta = a/6$ according to [5], rewriting everything in terms of the order parameter s, and including the Jacobian of the transformation, $dr_N/ds = Na$, we finally obtain

$$G_{\text{coil}}(s) = 3Ns \, \exp\left(-\frac{3}{2}Ns^2 - Nu\right)\left\{1 - \left(1 - \frac{L}{Na}\right) \\ \times \exp\left[-6\frac{L}{Na}\left(\frac{L}{Na} - s\right)\right]\right\}. \tag{22}$$

The maximum value of the order parameter in the coil state is achieved when the free end is just touching the edge of the piston.

The flower conformation is inhomogeneous, and only one part is stretched. The corresponding branch of the Landau free energy is written as

$$\Phi_{fl} = -\frac{1}{N}\ln[G_{\text{stem}}(n)Q_{\text{crown}}(N - n)]. \tag{23}$$

The stem is defined as a subchain starting from the anchored chain end and ending with the first segment to reach the edge of the pistons. Again, the Green's function of the stem has to be calculated with the vanishing boundary condition mentioned above. The result is well known [5] and for the case of cylindrical geometry of the space between two pistons has the following form:

$$G_{\text{stem}}(n) = 3\left(\frac{L}{na}\right)^3\exp\left(-\frac{3L^2}{2na^2} - nu\right). \tag{24}$$

The partition function of an $(N-n)$-segment chain end-fixed at the step potential u was calculated exactly in [23,24] and is given by

$$Q_{\text{crown}}(N - n) = \exp\left(-\frac{u(N - n)}{2}\right)I_0\left(\frac{u(N - n)}{2}\right) \tag{25}$$

where I_0 is the modified Bessel's function.

Expressed in terms of the order parameter the restricted partition function (with the proper Jacobian $dn/ds = L/s^2 a$) is given by
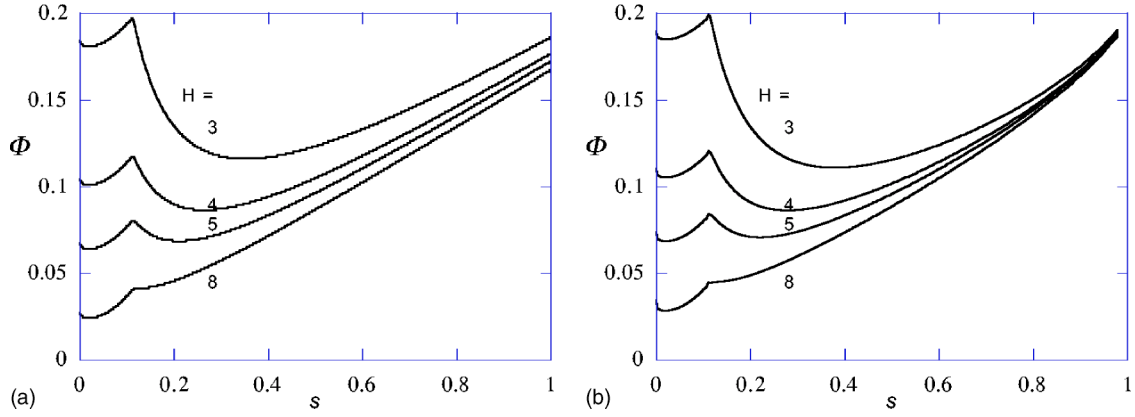
FIG. 9. The Landau free energy as a function of the order parameter for $L/a=90$, $N=800$ and various values of the confinement width $H=3$, 4, 5, and 8. (a) Analytical results for the Gaussian chain and (b) numerical freely jointed chain model.

$$e^{-N\Phi_{fl}(s)} = 3\frac{L}{a}s\,\exp\left(-\frac{uL}{2as} - \frac{3Ls}{2a} - \frac{uN}{2}\right)I_0\left(\frac{uN}{2} - \frac{uL}{2as}\right).$$

$$(26)$$

For the escape transition to have an abrupt character, the following conditions should be satisfied: $N\gg1$ and $uN\gg1$. Using the asymptotic representation of the modified Bessel's function and neglecting the terms of order N^{-1} one arrives at the following simple analytical expressions:

$$\Phi(s,H) \approx \begin{cases} \dfrac{3}{2}s^2 + \dfrac{1}{6}\left(\dfrac{\pi a}{H}\right)^2, & s \leq \dfrac{L}{Na} \\[3mm] \dfrac{3L}{2Na}s + \dfrac{L}{6Na}\left(\dfrac{\pi a}{H}\right)^2\dfrac{1}{s}, & s \geq \dfrac{L}{Na} \end{cases} \quad (27)$$

where we have expressed u in terms of the confinement width, H. Integrating over the order parameter according to Eq. (20), we can recover the partition functions for the coil and the flower states separately.

The conditions that we have used can be rewritten in terms of H in the form $R_g/H\gg1$, where R_g is the gyration radius of a nondeformed coil. It is clear that in this limit the two natural dimensionless parameters that define all aspects of the escape transition are the ratio of the confinement width to the segment length, H/a, and the ratio of the piston radius to the contour length of the chain, L/Na. The importance of this choice is due to the fact that both parameters serve as intensive variables in describing the escape transition.

The Landau free energy calculated according to Eqs. (22) and (26) is presented in Fig. 9(a) as a function of the order parameter for various values of the confinement width H and for fixed values $L/a=45$, $N=400$. It is clear that the two branches of the Landau function match each other at $s=L/Na$. Neither the shape of the coil branch nor the point where the two branches meet depend on the confinement width H, whereas the flower state branch is of course affected by it. With a decrease in H, the minimum in the flower branch becomes more pronounced. Changing H results also in an overall shift of the Landau free energy curve along the vertical axes, but this does not have any effect as far as the transition is concerned.

It is of considerable interest to discuss the relatively small differences between the Gaussian chain results, Fig. 9(a), and the freely jointed chain model, Fig. 9(b). Both results apply to the case that the excluded volume of the chains is ignored, however, the freely jointed chain has a finite extensibility of the chain and the Gaussian chain has not. The difference becomes relevant in the limit of strongly stretched chains. This means that this is the case for large values of the stretching parameter s. Indeed, inspection reveals that the curves become insensitive to the value of H for large s in the freely jointed chain model, whereas there remains a compression distance dependence in the Gaussian chain case. Near the transition, however, the finite extensibility effects are not important. The changes for small s values are due to the fact that the finite discretization used in the freely jointed chain model leads to artifacts for very small values of H.

C. Binodal and spinodal conditions

The minimum of the Landau function determines the average value of the order parameter in the (local) minimum of the system. The binodal condition is found when the two minima of the Landau function are equally deep. To simplify the analysis of the binodal and spinodal conditions we use the asymptotic expression (27) for the Landau free energy, as opposed to the exact equations illustrated in Fig. 9. Then, the compressed coil minimum is located at $s=0$ and has the depth of $\Phi(0) = \frac{1}{6}\left(\frac{\pi a}{H}\right)^2$. The minimum corresponding to the escaped flower state is found at $s_{esc} = \frac{\pi a}{3H}$, its depth being $\Phi(s_{esc}) = \frac{\pi L}{NH}$. This leads to the binodal condition of Eq. (5).

With the decrease in the confinement width, the escaped flower state becomes metastable. Once the height of the barrier separating this minimum from the stable equilibrium vanishes, metastability is lost. This happens when the position of the escaped state minimum s_{esc} coincides with the position of the barrier $s_0 = \frac{L}{Na}$. Thus the spinodal condition is given by

$$\frac{H^{**}}{a} = \frac{\pi}{3}\frac{Na}{L}, \qquad (28)$$

that is, metastability is lost completely when the confinement width is twice as small as given by the binodal line.

We mentioned earlier that the condition for the escape transition to be of abrupt nature is $R_g/H \gg 1$. Combined with the binodal equation, this leads to $L/R_g \gg 1$. It is clear that in this case the compressed coil state is metastable irrespective of the value of the confinement width, since the coil branch of the Landau function is unaffected by changes in H.

The compressed coil state will become unstable only if the radius of the piston is comparable to the gyration radius of coil. Formally, this condition is found by requiring that the barrier height in the Landau function (calculated for the whole chain) be equal to $1kT$:

$$\Phi(s_0) - \Phi(0) = N^{-1} \tag{29}$$

which yields

$$\left(\frac{L}{R_g}\right)^{**} = 2. \tag{30}$$

D. Barrier heights separating the stable and the metastable states

The analytical expressions for the Landau free energy allow us to compute the height of the barrier separating the coil and the escaped flower minima. The barrier height counted from the coil state minimum, in scaling variables, is simply given by

$$\Delta_{coil} = \tilde{L}^2 \tag{31}$$

and has the meaning of the elastic free energy of stretching the chain to the edge of the piston. The barrier height counted from the flower state minimum is equal to

$$\Delta_{fl} = (\tilde{H}^{-1} - \tilde{L})^2 \tag{32}$$

for $\tilde{H}^{-1} \gg \tilde{L}$. The spinodal condition corresponding to a vanishing barrier is written in the scaling variables as $\tilde{H}^{**} = \tilde{L}^{-1}$. From this it is possible to show that the barrier height depends on the proximity to the spinodal:

$$\Delta_{fl} = [\tilde{H}^{-1} - (\tilde{H}^{**})^{-1}]^2. \tag{33}$$

Finite-size correction to the spinodal condition given by Eq. (28) can be found by taking $\Delta_{fl} \sim 1$ which would give $(\tilde{H}^{-1})^{**} = \tilde{L} + 1$. A more careful consideration also reveals other finite-size corrections due to the difference between the exact expression for the partition function of the crown, given by Eq. (25) and its asymptotic representation that was used. As follows from the numerical analysis of the transition kinetics presented below, the actual spinodal condition for finite chains can be very accurately represented as

$$(\tilde{H}^{-1})^{**} = \tilde{L} + 1/2. \tag{34}$$

E. Phase diagram

Figure 10 displays the phase diagram drawn for a finite chain of length $N=800$. We show the binodal line $(L/Na)^* = \pi a/6H$ and the spinodal indicating the instability of the in
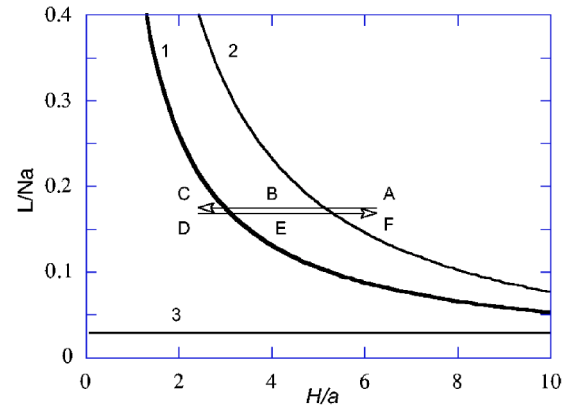

FIG. 10. Phase diagram including one binodal (1) and two spinodal lines (2) and (3) for $N=800$ in the $\tilde{L}/Na$ and H/a coordinates. The path following the points ABCDEF will be discussed in the text.

Eq. (30) and the spinodal line corresponding to the instability of the flower conformation. The latter spinodal is basically Eq. (28) including the finite-size effects following from Eq. (34) and has the form

$$\left(\frac{L}{Na}\right)^{**} = \frac{\pi a}{3H} - \frac{a}{6R_g}. \tag{35}$$

We stress that we are interested in studying the region of universal behavior, where the confinement width H should be at least a few segment lengths. The region of extreme compression $H<1$ (not shown in the diagram) was studied extensively by Ennis *et al.* [10]. Of course, under these conditions the compression entropy and the stem elasticity become strongly dependent on the details of the model used (lattice vs off-lattice, persistent vs freely jointed, etc., including the particulars of the single-segment bond potential).

It is clear then that L/Na ratio's allowing the escape transition to be observed are rather small: for $H=3$ we get $L/Na \approx 0.15$ at the binodal. Combined with the condition $L/2R_g > 4$ in order to have a fairly pronounced transition, this leads to a strong requirement on the minimum chain length: $N \geq 800$. For the chain length chosen ($N=800$), all the lines nearly merge together at $H \sim 10$, comparable to the gyration radius $R_g = 11.547$.

Metastable states and hysteresis effects will be observed as one moves along the path ABCDEF shown in the phase diagram (Fig. 10). The first part of the process (ABC) corresponds to a gradual compression of a chain initially residing in the confined coil state. If the compression proceeds quickly enough the chain remains in the coil state even though point C corresponds to the stable flower state. Once enough waiting time is allowed to reach the stable equilibrium, the chain partially escapes and thus the state at point D is not the same as at C. Now, the path is reversed (DEF) and the piston separation is gradually increased. At point E, one finds the metastable escaped flower, but after crossing the spinodal line 2, this state disappears, and points F and A are completely equivalent. The changes in the Landau free energy with decreasing H are shown in Fig. 9.

F. Transition kinetics

The spinodal condition and the hysteresis effects described above are actually of kinetic nature and depend on the ratio of a typical experimental measurement time and the internal relaxation time. It is well known that relaxation time for a process involving barrier crossing is exponential in the barrier height. Hence we expect the characteristic lifetime of a metastable coil to be of the order of $e^{\tilde{L}^2}$ independent of the confinement width H. For a metastable flower the lifetime is expected to be of the order of $\exp[\tilde{H}^{-1}-(\tilde{H}^{**})^{-1}]^2$. In this case, the barrier height is controlled by the proximity to the spinodal value of the confinement width H^{**}.

From the point of view of potential applications, the situation when the lifetime of the metastable state is not very large may be of particular interest. In this case the estimates based on the barrier height only become too crude. We apply the Fokker-Plank equation formalism to find a more accurate estimate for the characteristic decay time of the metastable states. A complete description of the coil-flower transition kinetics would require solving an equation in a $3N$-dimensional configuration space. However, since we are interested in the slowest process only, the problem is simplified drastically. Assuming that the slowest mode is associated with the relaxation of the order parameter and all the other degrees of freedom equilibrate quickly, we can write a one-dimensional Fokker-Plank equation for the probability density $P(s,t)$ with the Landau function $N\Phi(s)$ playing the role of the effective potential:

$$\frac{\partial}{\partial t}P(s,t) = \frac{\partial}{\partial s}D(s)\left[\frac{\partial P(s,t)}{\partial s} + P(s,t)N\frac{\partial \Phi(s)}{\partial s}\right]. \quad (36)$$

Here $D(s)$ is the diffusion coefficient along the configuration space path described by the order parameter s. The two branches of the Landau function $\Phi(s)$ are given by Eqs. (22) and (26).

The question of whether the relevant part of the full $3N$-dimensional dynamics can be adequately described by a reduced 1D equation was investigated very thoroughly by Muthukumar [26] for a problem of a polymer chain translocation though a hole in a wall. It was demonstrated that this reduction is remarkably successful, which provides confidence in the validity of the approach taken here.

Standard analysis [27] provides an expression for the mean first passage time τ_{coil}, i.e., the time required by the chain initially in the coil state to go to the top of the barrier is given by

$$\tau_{\text{coil}} = \int_{s_c}^{s_0} ds \frac{\exp[N\Phi_{\text{coil}}(s)]}{D(s)} \int_{-\infty}^{s} ds' \exp[-N\Phi_{\text{coil}}(s')] \quad (37)$$

where $s_c = 1/(\sqrt{2}\tilde{L})$ is the position of the coil minimum with finite-chain correction, and $s_0 = L/(Na)$ is the position of the barrier maximum. The usual way of dealing with this expression is to approximate the internal integral over s' by extending the upper limit of integration to s_0. Then, by definition of the Landau function, it has the meaning of the partition func-

tion of the coil state, Q_{coil}, which can be taken out of the integral over s. The diffusion coefficient $D(s)$ describes the dynamics in terms of the variable s. The conventional translational diffusion coefficient D for the center-of-mass coordinate of a free-draining chain is $D=(N\zeta)^{-1}$, where ζ is the friction coefficient per segment. Since the time required for a certain displacement is invariant with respect to changing the dynamic variable, $(ds)^2/D(s)=(dz)^2/D$. Recalling that $s=z/N$, one finds $D(s)=N^{-3}\zeta^{-1}$.

In the problem we are dealing with, one end of the chain is fixed, and the single dynamic variable is associated with the end-to-end distance. The diffusion coefficient to be ascribed to the free end differs from that associated with the center-of-mass motion by a numerical coefficient. This can be found by establishing a mapping onto the well-known solution [27] for the fundamental relaxation time of the Rouse chain with one end fixed: $\tau_{\text{Rouse}}=(4/3\pi^2)N^2a^2\zeta$. The relaxation time of the x component of the end-to-end distance taken as a single Gaussian degree of freedom with a diffusion coefficient D is simply $\tau=(KD)^{-1}$, where $K=3/Na^2$ is the elastic coefficient. Identifying this result with τ_{Rouse} gives $D=(\pi^2/4)(N\zeta)^{-1}$. Since the time required for a certain displacement is invariant with respect to changing the dynamic variable, $(ds)^2/D(s)=(dz)^2/D$. Recalling that $s=z/(Na)$, one finds $D(s)=\pi^2(4N^3a^2\zeta)^{-1}$.

The exponential term $\exp[N\Phi_{\text{coil}}(s)]$ is simply the inverse of the Green's function [cf. Eq. (21)].

$$\tau_{\text{coil}} = \tau_{\text{Rouse}}\frac{Na^2}{3L^2}\exp\left(\frac{3L^2}{2Na^2}\right)\left[1 - \frac{1}{2}\ln\left(\frac{L}{Na}\right)\right]. \quad (38)$$

A comparison with the direct numerical evaluation of Eq. (37) shows that the analytical expression Eq. (38) is very accurate almost up to the spinodal.

In the formulation of the escape problem, the control parameter is the piston separation. In the phase diagram, this corresponds to moving along a horizontal path. We note that in this process, the coil lifetime does not depend on the piston separation (this is only true for ideal Gaussian chains). The exponential factor contains the barrier height Δ_{coil}, see Eq. (31), which is determined by the initial choice of the piston radius and the chain length. If this choice is such that the system is close to the coil spinodal line, $L/R_g \lesssim 2$, the metastable coil decays with a typical Rouse relaxation time which is of the same order of magnitude as all the other characteristic times for the motion of the chain as a whole: for realistic chains with the number of segments $N=500-1000$ this is of order of milliseconds. For larger L/R_g ratios, the decay time may be considerably longer, as illustrated by Fig. 11. For example, if $L/R_g=8$, the coil lifetime is estimated to be of the order of hours.

The mean first passage time for the chain initially in the flower state, τ_{fl}, is given by a similar expression:

$$\tau_{fl} = \int_{s_0}^{s_{fl}} ds \frac{\exp[N\Phi_{fl}(s)]}{D(s)} \int_{s}^{\infty} ds' \exp[-N\Phi_{\text{coil}}(s')]. \quad (39)$$

The relevant diffusion coefficient $D(s)$ is more difficult to interpret since the chain is in an inhomogeneous conforma-
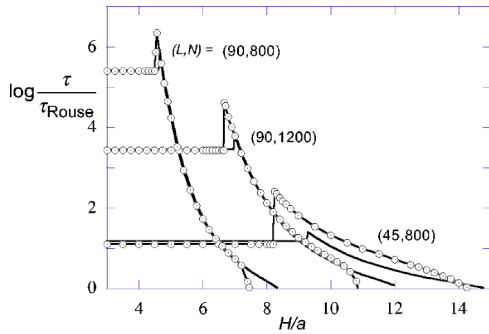
FIG. 11. The normalized mean first passage time τ/τ_{Rouse} of the metastable flower (large H) and the metastable coil (small H) in logarithmic coordinates as a function of the confinement distance H. The lines marked by the points are found from numerical integration of the Fokker-Plank equation with the exact Landau function (no approximations), and the transition point determined from the actual Landau functions. The lines without the marks are results obtained from calculations according to the analytical asymptotic formulas (and the transition point is calculated from the asymptotic analytical expression). The values of L and N are indicated.

tion. However, the main contribution to the integral comes from the barrier region where the stem comprises almost all of the chain. The total friction coefficient of a uniformly stretched chain with one end fixed is simply $N\zeta/2$. It follows that $D(s)$ should be taken as $D(s)=2N^3\zeta^{-1}$ (which is very close to what was used earlier).

Asymptotic evaluation of the integral provides the following expression:

$$\tau_{fl} \cong \tau_{\text{Rouse}} \frac{\pi}{\sqrt{2}} \tilde{L}\tilde{H}W\left(\frac{\tilde{H}^{-2}-\tilde{L}^2}{2\tilde{H}^{-1}}\right)\exp(\tilde{H}^{-1}-\tilde{L})^2 \quad (40)$$

where $W(x)=\exp(-x^2)\int_0^x \exp(t^2)dt$ is the Dawson integral. The lifetime contains the expected exponential factor, $\tau_{fl} \sim \exp(\Delta_{fl})$.

Figure 11 displays the lifetimes of metastable states as a function of the confinement width, H, for several chain lengths and piston radii. Below the transition point, $H<H^*$, the lifetime of a metastable coil is independent of the confinement width (this is, of course, valid only for ideal chains considered here). Above the transition point, the lifetime of the metastable flower state decreases until the escaped part disappears completely. At the transition point the two branches do not match, which is due to an asymmetry of the barrier shape. The difference lies in the preexponential factor. Since the first passage time is calculated for the path from the bottom of the well to the top of the barrier (and not to the bottom of the other well) there is no contradiction with the detailed balance argument that would require equal transition times for equally probable states. Comparing the results of numerical integration with exact Landau functions (dots) and the asymptotic analytical expressions (solid lines) we notice that (apart from a small shift on the H axis) the latter provide excellent agreement except for the close vicinity of the spinodal where τ_{fl} becomes close to or less than the Rouse relaxation time. In this case the time of the first barrier

crossing becomes comparable to the time required to get from the top of the barrier to the stable minimum, which is again of the order of τ_{Rouse}.

It is useful to give some numerical estimates in order to get a feeling of the time scales involved. The elementary relaxation time of a segment is typically on the order of several nanoseconds, 10^{-8} s. This is what is seen, e.g., in polarized luminescence. Then, the Rouse time will be $\sim 10^{-3}-10^{-2}$ s for N in the range of $400-1200$. Figure 11 demonstrates a very strong chain length effect on the equilibration time in the vicinity of the binodal point for a fixed value of the piston radius. Again, this effect is, to a certain extent, counterintuitive: for a longer chain with $N=1200$, the relaxation time will be on the order of 10 s; for a slightly shorter chain with $N=800$, the relaxation time increases to about an hour, while for $N=400$ (not shown) it is measured in days. Again this result is attributed to the increase in N/L values.

VI. DISCUSSION

The escape transition refers to an abrupt conformational change from a coil-like state to an inhomogeneous flower state as a result of squeezing the polymer chain between two pistons. The coil-to-flower transition occurs also in other situations, namely, when an end-fixed chain is placed near a liquid–liquid or solid–liquid interface. It was proved that all these models are mathematically equivalent for ideal chains [19]. Within the class of equivalent models demonstrating the coil-to-flower transition, all the results can be easily transferred from one model to another. In particular, for the adsorption problem we have performed the analysis in terms of the Yang-Lee theory that relates the phase transition characteristics to the distribution of zero's of the partition function in the complex plane of the control parameter. In the present paper, we did not intend to discuss this approach in any detail. However, the formulated analogy allows us to state very confidently that all the features of the complex zero distribution in the escape problem remain the same as in [22].

At this junction we stress once again that the phase transitions of the coil-to-flower type are rather unique. This is due to the fact that not only the exact partition function can be found for finite-size systems, but also the Landau free energy containing all the information on the metastable states. The main reason is that the appropriate order parameter is justifiably defined globally and the fluctuations of the order parameter can be calculated exactly. Thus the Landau free energy is not a functional but a simple function.

Note that not all single-chain phase transitions are naturally described in terms of a global order parameter. For instance, in the coil-globule transition the order parameter is simply the local monomer density. Correspondingly, the kinetics of the collapse of a coil is governed by the growth and coalescence of multiple nucleation centers, and the initial stages do not necessarily involve any change in the large-scale conformation of the coil. As opposed to that, in the escape transition the new (escaped) phase emerges via a single nucleus when the free end of the chain reaches the

piston edge and forms a seed crown of one or just a few segments; its appearance involves a global change in the chain conformation. This nucleus is at the top of the nucleation barrier, and therefore we have to associate this state with the critical nucleus. Note that there is no simple direct analogy for a stable phase nucleus with a smaller than critical size: In fact such conformation is just in the metastable configuration, even though it is deformed and therefore away from the metastable minimum. Hence, contrary to the standard picture of nucleation in classical systems, the critical nucleus remains the same irrespective of the external parameters (or the position in the phase diagram), as long as the metastable state does exist. Of course, the nucleation barrier height does depend on the external parameters, and is determined by either the stretching free energy alone (for the metastable coil) or by its competition with the free energy of compression (for the metastable flower). The picture of the critical nucleus remains exactly the same in other coil-to-flower transitions induced by a stepwise external potential [5] or an adsorbing surface [22].

Once again, it is the fact that the escape transition is adequately described in terms of a single global order parameter that allows one to construct a simple theory for both equilibrium and kinetic aspects of this phenomenon. The nature of the order parameter also dictates the basic mechanism leading to a decay of an unstable state within the spinodal region. For the coil-to-flower transitions, the unstable state is destroyed by a global conformation change with a simple Rouse relaxation time.

Experiments aimed to study these phase transitions may provide a unique insight into the problem of metastability and its relation to first-order phase transitions. Experiments in single-chain conformational phase transitions became more feasible with the advent of atomic force microscopy (AFM) [28–33]. Preparing the actual slit-like geometry with pistons of a radius of a few nanometers and confining a tethered chain in the gap is quite challenging. A perhaps simpler version could be realized for an equivalent coil-to-flower transition involving a solid adsorbing surface.

Although the Landau theory serves as a conceptual basis for understanding phase transitions, the systems allowing an explicit calculation of the Landau function are limited to very few examples. Two textbook cases are the Ising ferromagnetic and the Mayer-Saupe theory [34] of isotropic-nematic transition [35], both calculated in the mean-field approximation. In polymer physics, we have recently introduced exactly solved models for adsorption of an end-fixed Gaussian chain on liquid–liquid [5] and liquid–solid interfaces [22]. It was the analysis in terms of the Landau function that demonstrated the mathematical equivalence of these two models and the escape problem. The analogy proved to be very fruitful since it allows one to present the partition function for the escape problem in a closed analytical form.

VII. CONCLUSIONS

A careful analysis of the exact partition function of the Gaussian chain squeezed between two cylinders reveals detailed insight in the thermodynamic behavior of the system. Unusual in this system is the fact that the finite size effects that influence the phase transition are of considerable relevance for experimental reasons. Both equilibrium as well as kinetic aspects were analyzed in detail. From differentiation of the partition function we obtained both the compression as well as the lateral force as a function of the separation between the two pistons. In addition to this the average number of confined segments and its fluctuations were analyzed. In the thermodynamic limit these characteristics show jump-like behavior which corresponds to the first-order character of the escape transition. In the transition region we showed the importance of choosing the type of ensemble. Only for small systems the difference between the ensembles disappears. To describe the metastable states we analyzed the Landau free energy as a function of the stretching which has been identified as the global order parameter of the system. From this it is straightforward to point to the spinodal(s) of the system and information on the barrier heights separating local and global minima. The Landau free energy is used in a one dimensional Fokker-Plank equation to predict the lifetime of the metastable states. All our results are obtained for ideal chains. However, we expect the results to remain qualitatively valid for real chains. Our analysis is expected to be a useful guide for experimental work on single chain conformational phase transitions, e.g., by atomic force microscopy (AFM). Computer experiments in the form of detailed molecular dynamics simulations may be useful to verify our dynamic approach.

APPENDIX: FREELY JOINTED CHAIN MODEL

In a freely jointed chain (FJC) one considers the chain to be composed of segments with ranking number $s = 1, \ldots, N$. The bonds between neighboring segments have a fixed length and therefore the model differs from the Gaussian chain in several subtle ways. One important one is that the FJC has a finite extensibility. Typically, but not necessarily, the model is elaborated on a lattice and then there are only a limited number of places the next segment can go to. All these possible places obtain in principle the same statistical weight. In this work a cylindrical coordinate system of lattice sites is used. Introducing the coordinate z along the long axis of the lattice with lattice numbers $z = -M_z, \ldots, -1, 0, 1, \ldots, M_z$. In each layer z there are lattice sites in the radial direction $r = 0, \ldots, M_r$. Each ring (z, r) is the locus of a mean-field approximation where all governing parameters are homogeneous. The number of lattice site $L(z, r)$ is a function of r and given by $L(z, r) = \pi[r^2 - (r-1)^2]$. The normalized contact area of a lattice site at coordinate r with sites at $r+1$ is given by: $a(z, r) = 2\pi r / L(z, r)$. In this cylindrical co-

ordinate system we assume a simple cubic lattice in the limit of large r value. This means that there exists a limiting step probability to go from one layer to a neighboring one which is $\lambda = 1/6$. For finite values of r the transition probabilities depend on the value of r because of the lattice symmetry.

$$
\lambda_{ij}(r) = \begin{pmatrix} \lambda_{-1-1}(r) & \lambda_{-10}(r) & \lambda_{-11}(r) \\ \lambda_{0-1}(r) & \lambda_{00}(r) & \lambda_{01}(r) \\ \lambda_{1-1}(r) & \lambda_{10}(r) & \lambda_{11}(r) \end{pmatrix}
$$
$$
= \frac{1}{6} \begin{pmatrix} 0 & 1 & 0 \\ a(r-1) & 4-a(r)-a(r-1) & a(r) \\ 0 & 1 & 0 \end{pmatrix} \quad \text{(A1)}
$$

where $i = z' - z = -1, 0, 1$ and $j = r' - r = -1, 0, 1$ sample the neighboring sites of (z, r). Not all combinations of the values of i and j obtain finite step probabilities because diagonal steps are excluded.

The freely jointed chain end point distribution functions are easily generated on this lattice using a propagator formalism. We are going to assume that the chain is grafted with one of its ends to the coordinate $(0,0)$. This point is just halfway between the two surfaces of the piston. For convenience we introduce the piston operator $\delta_{z,r}$ which is zero when at site (z,r), the piston is present and unity otherwise. For example when $H = 5$ and $L = 10$ we have $\delta_{z,r} = 0$ for $(z,r) \in [|z| > 2 \cap r < 11]$ and unity elsewhere.

$$
G(z,r,s) = \begin{cases} 0 & s=1, z \neq 0, r \neq 0 \\ 1 & s=1, z=0, r=0 \\ \sum_{i,j} \lambda_{i,j}(r) G(z-i, r-j, s-1) \delta_{z,r} & s>1. \end{cases}
$$
$$
\text{(A2)}
$$

This means that the start of each walk (with segment $s=1$) is forced to be at the origin and the $\delta_{z,r}$ ensures that all walks that enter into one of the pistons are deleted.

The sum over all end points of walks with $N-1$ steps (N segments) gives the exact partition function:

$$
Q(H,L,N) = \sum_z \sum_r L(z,r) G(z,r,N). \quad \text{(A3)}
$$

To compute the Landau functions for the coil and flower, respectively, it is necessary to solve problems with slightly modified boundary and initial conditions. For example, for the coil one it is necessary to know the statistical weight to start at $(0,0)$ and ending at (z,r) without leaving the gap once. This property is computed by closing the cylinder opening at the edge. This is done by adjusting the piston operator, which in this case produces $0'$ for all $r > L$ as well, in addition to the piston coordinates specified above. We obtain $G'(z,r,N)$ where the prime indicates the closed gap boundary condition. The partition function is found after integration over all coordinates (z,r) similarly as in Eq. (A3).

The subpartition function for the stem of the flower is extracted easily. The stem reaches after $n-1$ steps the edge of the cylinder for the very first time and $G'(z,L,n)$ is the result for the statistical weight. The partition function for the crown that starts at the piston edge is easily found by modifying the initial condition of the walk with $N-n$ segments now starting not at $(0,0)$ but at $(0,L)$, where we assume that there are no strong gradients in the z direction. Note that in this case the gap is open and the chain is free to reenter the gap. The corresponding end-point distribution function $G''(z,r,N-n)$ is easily integrated over all (z,r) coordinates to obtain $Q_c(N-n)$. The flower with n segments in the stem has now probability $Q(H,L,n) = G'(z,L,n)Q_c(N-n)/(2\pi LH)$, where the normalization $2\pi LH$ is necessary to connect the stem to the crown.

In Fig. 1 results are presented for the coil escaping from an external potential as well as adsorbing onto a solid surface. In these systems again a cylindrical coordinate system is applied, and the chain is grafted by one end on a coordinate on the long axis $(z',0)$. In the adsorption problem the flat surface is positioned on some coordinate $z = z' + L$, i.e., a distance L away from the grafting point, and an adsorption energy gain is assigned to each segment that visits the layer next to the impenetrable surface. In the step potential problem the chain is again grafted at the long axis of the cylinder at $(z',0)$. Around the coordinate an unfavorable external potential is implemented, such that only on coordinates with $z > z' + L$ it can escape from the applied potential.

[1] P. J. Flory, *Principles of Polymer Chemistry* (Cornell Univ. Press, Ithaca, 1953).

[2] G. des Cloizeaux and J. Jannink, *Polymers in Solution Their Modeling and Structure* (Clarendon Press, Oxford, 1990).

[3] P. G. de Gennes, *Scaling Concepts in Polymer Physics* (Cornell Univ. Press, Ithaca, 1979).

[4] A. Y. Grosberg and A. R. Khokhlov, *Statistical Physics of Macromolecules* (Oxford University Press, New York, 1994).

[5] A. M. Skvortsov, L. I. Klushin, J. van Male, and F. A. M. Leermakers, J. Chem. Phys. **115**, 1586, (2001).

[6] E. Eisenriegler, *Random Walks in Polymer Physics, Lecture Notes in Physics*, Vol. 508 (Springer, New York, 1998).

[7] G. J. Fleer, M. A. Cohen Stuart, J. M. H. M. Scheutjens, T. Cosgrove, and B. Vincent, *Polymers at Interfaces* (Chapman and Hall, London, 1993).

[8] G. Subramanian, D. R. M. Williams, and P. A. Pincus, Europhys. Lett. **29**, 285 (1995).

[9] G. Subramanian, D. R. M. Williams, and P. A. Pincus, Macromolecules **29**, 4045 (1996).

[10] J. Ennis, E. M. Sevick, and D. R. M. Williams, Phys. Rev. E **60**, 6906 (1999).

[11] M. C. Guffond, D. R. M. Williams, and E. M. Sevick, Langmuir **13**, 1591 (1997).

[12] F. A. M. Leermakers and A. A. Gorbunov, Macromolecules

35, 8640 (2002).

[13] A. Milchev, V. Yamakov, and K. Binder, Phys. Chem. Chem. Phys. **1**, 2083 (1999).

[14] A. Milchev, V. Yamakov, and K. Binder, Europhys. Lett. **47**, 675 (1999).

[15] B. M. Steels, F. A. M. Leermakers, and C. A. Haynes, J. Chromatogr., B: Biomed. Appl. **743**, 31 (2000).

[16] E. M. Sevick and D. R. M. Williams, Macromolecules **32**, 6841 (1999).

[17] D. R. M. Williams and F. C. MacKintosh, J. Phys. II **9**, 1417 (1995).

[18] J. Jimenez and R. Rajagopalan, Langmuir **14**, 2598 (1998).

[19] A. M. Skvortsov, L. I. Klushin, and F. A. M. Leermakers, Europhys. Lett. **58**, 292 (2002).

[20] H. S. Carslaw and J. C. Jaeger, *Conduction of Heat in Solids* (Oxford, New York, 1947).

[21] E. Eisenriegler, K. Kremer, and K. Binder, J. Chem. Phys. **77**, 6296 (1982).

[22] L. I. Klushin, A. M. Skvortsov, and F. A. M. Leermakers, Phys. Rev. E **66**, 036114 (2002).

[23] A. M. Skvortsov, J. Van Male, and F. A. M. Leermakers, Physica A **290**, 445 (2001).

[24] A. M. Skvortsov, L. I. Klushin, J. van Male, and F. A. M.

[25] L. D. Landau and E. M. Lifshitz, *Statistical Physics* (Nauka, Moscow, 1976).

[26] M. Muthukumar, Phys. Rev. Lett. **86**, 3188 (2001).

[27] M. Doi and S. F. Edwards, *The Theory of Polymer Dynamics* (Clarendon Press, Oxford, 1986).

[28] B. J. Haupt, J. Ennis, and E. M. Sevick, Langmuir **15**, 3886 (1999).

[29] W. Baumgartner, P. Hinterdorfer, W. Ness, A. Raab, D. Vestweber, H. Schindler, and D. Drenckhahn, Proc. Natl. Acad. Sci. U.S.A. **97**, 4005 (2000).

[30] T. Hugel, M. Grosholz, H. Clausen-Schaumann, A. Pfau, H. Gaub, and M. Seitz, Macromolecules **34**, 1039 (2001).

[31] T. J. Senden, Curr. Opin. Colloid Interface Sci. **6**, 95 (2001).

[32] T. Hugel and M. Seitz, Macromol. Rapid Commun. **22**, 989 (2001).

[33] W. K. Zhang, S. Zou, C. Wang, and X. Zhang, J. Phys. Chem. B **104**, 10258 (2000).

[34] P. M. Chaikin and T. C. Lubensky, *Principles of Condensed Matter Physics* (Cambridge University Press, Cambridge, England, 2000).

[35] P. G. de Gennes and J. Prost, *The Physics of Liquid Crystals* (Clarendon Press, Oxford, 1993).

Leermakers, J. Chem. Phys. **112**, 7238 (2000).